Establishment of papillomavirus infection is enhanced by promyelocytic leukemia protein (PML) expression

Patricia M. Day*, Carl C. Baker, Douglas R. Lowy, and John T. Schiller

Laboratory of Cellular Oncology, Center for Cancer Research, National Cancer Institute, National Institutes of Health, Bethesda, MD 20892

Edited by Kenneth I. Berns, University of Florida, Gainesville, FL, and approved August 24, 2004 (received for review June 14, 2004)

Previous studies have suggested that most papillomaviruses enter the host cell via clathrin-dependent receptor-mediated endocytosis but have not addressed later steps in viral entry. To examine these events, we followed the localization of L2 and packaged DNA after entry of infectious virions or L1/L2 pseudovirions. Confocal microscopic analyses of HeLa cells showed a time-dependent uncoating of capsids in cytoplasmic vesicles and the accumulation of both L2 and viral DNA at distinct nuclear domains identified as nuclear domain 10 (ND10). Both L2 and the pseudogenome had a punctate distribution and localized to ND10 in promyelocytic leukemia protein (PML)-expressing cells, whereas L2 had a diffuse nuclear distribution in PML−/− cells. The number of pseudovirus-infected cells was an order of magnitude higher in the PML+ cells compared with the PML−/− cells, and viral genome transcription after infection with authentic bovine papillomavirus virions was similarly elevated in PML+ cells. The results identify a role for PML in the enhancement of viral infectivity in the early part of the life cycle. We propose a model in which L2 chaperones the viral genome to ND10 to efficiently initiate viral transcription.

To protect their genome from degradation by external factors, viruses mature by surrounding their nucleic acid with a proteinaceous coat. Conversely, after adsorption and penetration into a host cell, viruses must undergo a controlled process of uncoating to render the genome accessible to the cellular components necessary for initiating viral gene expression and the replicative cycle. DNA viruses, excluding poxviruses, have the additional onus of delivering their genetic material into the nucleus to allow access to the host cell transcriptional machinery.

The nuclear homing of karyophilic viral particles during natural infection can occur by various mechanisms (reviewed in ref. 1). Small virions, such as those from hepatitis B virus (2), can pass intact directly through the nuclear pore complex (NPC). Simian virus 40 also appears to transit the NPC in intact form despite its 50-nm size (3), although an alternate route into the nucleus cannot be excluded. However, the interior diameter of the central NPC channel prevents the capsids of most nuclear viruses from entering without at least partial disassembly of the virion. Adenoviral capsids complete their dissociation at the NPC with nuclear delivery of protein VII and viral DNA (4). The capsids of HSV-1 also dock at the nuclear pore and extrude their DNA into the nucleus (5).

After entry into the nuclear milieu, initial viral transcription must be stimulated either by finding a location in a preexisting transcription environment or by recruiting the essential factors. The viral genomes of several DNA viruses have been shown to localize and initiate their RNA synthesis in the vicinity of distinct nuclear regions known as nuclear domain 10 (ND10), also referred to as promyelocytic leukemia protein (PML) nuclear bodies or PML oncogenic domains (PODs), which are discrete interchromosomal accumulations of several proteins, including PML and Daxx (reviewed in ref. 6). However, the role of ND10 in this process is unclear. Most DNA viruses, including herpesviruses and adenoviruses, have evolved mechanisms to disrupt ND10 early in their replicative phase (reviewed in refs. 7 and 8), and the absence of this ability can adversely affect the success of the infection (9), suggesting a negative role for ND10 in viral gene expression. Many ND10 proteins are IFN-inducible (10–13), lending further credence to a role in antiviral defense.

The papillomaviruses (PVs) are nonenveloped icosahedral DNA viruses that induce benign epithelial papillomas and have been implicated etiologically in human cervical carcinoma, as well as in a subset of other epithelial carcinomas (14). Two proteins comprise the PV protein shell: the major capsid protein, L1, which can self-assemble into noninfectious virus-like particles; and the minor capsid protein, L2, which is essential for infectivity. L2 has been implicated in viral DNA encapsidation for many PV types, including bovine PV (BPV), which is a standard PV for *in vitro* studies (15, 16). L2 also serves a less well defined role in an early event in the infectious process, because BPV L2 mutants have been described that produce noninfectious viral particles containing wild-type levels of encapsidated viral genome (17).

Most PVs enter the host cell via clathrin-dependent receptor-mediated endocytosis (18–20). However, these analyses have not addressed the later steps in viral entry, namely where viral uncoating may begin, whether either capsid protein accompanies the viral genome into the nucleus, or the site within the nucleus at which the viral genome initiates its transcription. To examine these events, we have developed two technologies by using PV pseudoviruses, defined here as vectors composed of both capsid proteins that transduce an encapsidated reporter plasmid, hereafter referred to as a pseudogenome. First, we produced infectious pseudoviruses carrying an epitope-tagged L2 protein, allowing us to track L2 after viral entry. We then developed a method for following the packaged viral pseudogenome by labeling it with BrdUrd, which permits the simultaneous detection of the pseudogenome and L2 with antibodies specific for BrdUrd and hemagglutinin (HA), respectively. Our results support a model whereby uncoating is initiated in cytoplasmic vesicles, followed by the papillomaviral L2 protein mediating the delivery of the viral genome into the nucleus to ND10. In apparent contrast to other DNA viruses, the presence of ND10 is associated with enhanced papillomaviral transcription.

Materials and Methods

Plasmids. The plasmids used for pseudovirus production have been previously described: BPV L1 pAL, BPV L2 PML, HPV16 L1, HPV 16 L2, and packaging plasmids pYSEAP and pSU-5697 (21, 22). To create the HA epitope-tagged L2 construct, bL2HA, the previously described vector PMLH was digested with the restriction endonucleases *Sph*I and *Xba*I and ligation of the annealed and likewise digested primers, 5′-CGACATGCATG-CAGCGTAGTCTGGGACGTCGTATGGGTATAATCT-AGACTAGT-3′ and its reverse complement. The sequence was confirmed on both strands. The *PML3* gene, a kind gift of Pier Giuseppe Pelicci (European Institute of Oncology, Milan), was transferred into the pIRES-hygro2 vector (Clontech).

This paper was submitted directly (Track II) to the PNAS office.

Abbreviations: ND10, nuclear domain 10; PV, papillomavirus; BPV, bovine PV; PML, promyelocytic leukemia protein; HA, hemagglutinin; QRT-PCR, quantitative RT-PCR.

*To whom correspondence should be addressed. E-mail: pmd@nih.gov.

Cell Lines. PML−/− murine embryo fibroblasts were a kind gift of Pier Paolo Pandolfi (Memorial Sloan–Kettering Cancer Center, New York) (23). These cells were grown in DMEM supplemented with 10% FBS and 500 μg/ml G418. The Hemp- and HP3-derived cell lines were obtained via transfection by electroporation with either empty vector or PML3-containing vector, respectively. Transfectants were selected with 400 μg/ml hygromycin. Resistant colonies were grown as bulk cultures. 293TT (21) and HeLa cells were grown in DMEM supplemented with 10% FBS and antibiotics.

Viruses. BPV-1 virions were purified from warts by standard techniques (16). BPV-1 pseudovirus was made and purified as described (21). Briefly, BPV L1 and a packaging plasmid were transfected into 293TT cells along with the plasmid encoding the wild-type L2 protein or the L2-HA fusion protein. Pseudovirus was purified 48 h posttransfection by centrifugation through an Optiprep (Sigma) gradient. To obtain packaged BrdUrd-labeled DNA, 20 mM BrdUrd was added to the producer cells at 6 h posttransfection during pseudovirion production. For BrdUrd-labeled pseudovirus, the plasmid PYSEAP was routinely used. Infectivity of pseudovirus with packaged pSU-5697, a GFP-expression plasmid, was determined by flow cytometric analysis 48 h postinfection on a FACSCalibur flow cytometer (Becton Dickinson).

Microscopy. Cells were seeded onto glass coverslips in a 24-well plate at a density of $6 \times 10^4 - 1 \times 10^5$ per well. Pseudoviruses were added for the time indicated in the text. L2 was detected with anti-HA reagents from Babco (Richmond, CA). BrdUrd was detected with BrdUrd labeling and detection kit I (Roche Diagnostics). PML was detected with a rabbit polyclonal antiserum (Chemicon). Fluorescence was examined with a Bio-Rad MRC 1024 laser-scanning confocal system attached to a Zeiss Axioplan microscope. The use of control coverslips established that fluorescent emissions in the green and red channels were not overlapping, and that antibody binding was for the intended antigen. The images were collaged and subjected to scale adjustment with ADOBE PHOTOSHOP software (Adobe Systems, San Jose, CA).

RT-PCR. Purified virions were added to 10^6 cells, and the infection was allowed to progress for 3 days. RNA was prepared by using the kit RNAqueous (Ambion, Austin, TX) and DNase treated by using the Ambion DNA-free DNase Treatment and Removal Reagent.

Spliced BPV-1 mRNA was quantified by using splice-specific real-time quantitative RT-PCR (QRT-PCR), as described (24). The primer pair oCCB-486: CCTCGATTTGTACTTGCATAGTC and oCCB-481: GTCTGGGCGATCTCCG was designed to amplify only the viral early protein 5 (E5) mRNA transcribed from the P2443 promoter and spliced from nucleotides 2505–3225 (25). This primer pair gives no signal in real-time PCR tests using 10 pg of BPV-1 genomic DNA as template, indicating it is specific for spliced mRNA.

For two-step RT-PCR analysis, RNA was first reverse transcribed to cDNA by using the Bio-Rad iScript cDNA Synthesis Kit with 1 μg of RNA in a 20-μl reaction. Real-time QRT-PCR assays were carried out on a Bio-Rad MyiQ Single-Color Real-Time PCR Detection System (Bio-Rad) by using the Bio-Rad iQ SYBR Green Supermix, with 300 nM primers and 1 μl of template (RT reaction or control plasmid) per 25 μl of PCR and an annealing temperature of 55°C. Melt curve analyses were performed on all PCRs to rule out nonspecific amplification. Standard curves were created for each run by using 10-fold serial dilutions of p753–1, a cDNA clone for the BPV-1 E5 mRNA (26). Data are expressed as femtogram of the DNA standard. Reactions were performed in triplicate.

Results

Characterization of HA-Tagged L2 Fusion Protein and BrdUrd-Labeled Pseudoviral Genome. Our first goals were to examine the nuclear entry of the PV genome and its possible continued association with L1 and/or L2 as well as where in the cell the initial uncoating took place. We expected that at least partial disassembly of the viral particle would occur before nuclear import, because it has been reported that intact human PV capsids are unable to enter the nucleus (27, 28). Consistent with this possibility, initial analyses of HeLa cells infected with BPV-1 virus or pseudovirus showed no evidence of nuclear L1 with any of several tested L1 antibodies or fixation conditions (data not shown). However, the accumulation of nuclear L2 was detected with a number of polyclonal antisera after acetone fixation (data shown as Fig. 6, which is published as supporting information on the PNAS web site).

Unfortunately, we found that acetone fixation was incompatible with our method for pseudogenome detection, which would prevent us from determining whether the pseudogenome and L2 showed intranuclear colocalization. To circumvent this problem, we constructed an L2 gene encoding a C-terminally HA-tagged protein, because antibodies to this epitope are widely available, and a short peptide epitope is less likely to be constrained by fixation procedures. Another benefit of this approach is that placement of the epitope at this site should allow accessibility to the HA antibody only after uncoating has begun, because the C terminus of L2 is not displayed on the surface of PV virions (29). The correlation of internalized virus to infectious events is usually complicated by the fact that most viruses have high particle-to-infectivity ratios, implying that the majority of the incoming particles do not result in establishment of infection. Therefore, it can be difficult to distinguish the trafficking of noninfectious particles from those that establish infection. This problem would be partially alleviated by detection of only uncoated particles, a step that is necessary but probably not sufficient for the establishment of viral infection. Monitoring when an epitope located internally on the virion becomes accessible to antibody staining would also allow us to assess the timing and localization of disassembly events.

Transfection of the HA-tagged L2 construct resulted in high expression of L2 and colocalized staining with anti-L2 and -HA reagents (data not shown). In addition, the presence of the HA moiety in the L2 protein did not impair its ability to participate in the production of infectious pseudovirus, as determined by its packaging a GFP expression plasmid and assessing the infectivity of the progeny pseudovirus (Fig. 1). These results suggested it would be possible to monitor the trafficking of infectious pseudovirus and to identify the input L2 protein and pseudogenome simultaneously. To detect the viral pseudogenome with high sensitivity, we added BrdUrd to the culture during pseudovirus production. The purified, labeled pseudovirus particles were then added to target cells to mimic the infectious entry process, and the input pseudogenome was detected with an anti-BrdUrd antibody. After pseudovirus purification, preliminary experiments demonstrated that the nuclease-resistant encapsidated pseudogenome was the only BrdUrd-labeled nucleic acid available for detection, and that it was not accessible to antibody detection while enclosed in the intact viral particle (data not shown and Fig. 2).

Time Course of Viral Uncoating. As expected, the initiation of infection led to a time-dependent increase in the detection of both the HA-tagged L2 protein and the viral pseudogenome. This result indicated that the detection of both components occurred only after some pseudovirus disassembly had occurred. The initial uncoating, as evidenced by anti-HA staining, was detected in cytoplasmic vesicles by 6 h of infection (Fig. 2), with

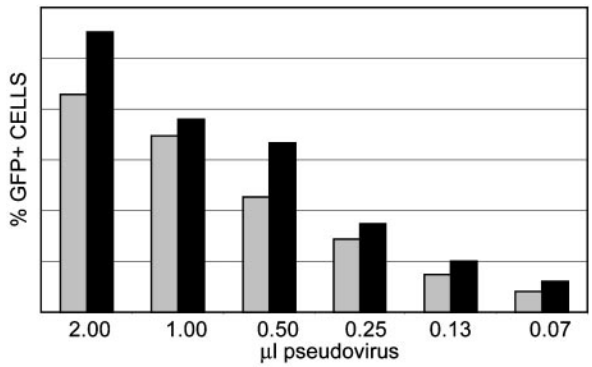

Fig. 1. Pseudovirus assembled with an HA-tagged L2 protein is infectious. Pseudovirus assembled with BPV L1 and either wild-type BPV L2 (gray bars) or L2-HA (black bars) and the GFP-expressing packaged plasmid pSU-5697 were used to transduce 293TT cells. Equivalent amounts of purified virus were purified. One microliter of virus is ≈1 μg of virus. Input virions were titrated and added to cells for 48 h. GFP fluorescence was determined by flow cytometric analysis. Marker boundaries were set such that untransduced control cells showed <1.0% fluorescent cells.

an increase in vesicular staining developing during the subsequent period of incubation. The observed lack of reactivity at the 2-h time point (Fig. 2*B*) reinforces the conclusion that epitope availability depends upon disassembly. By 20 h after infection, the nuclear entry of pseudogenome and L2 was clearly evident, and by 24 h, ≈30% of the cells showed a punctate nuclear pattern. Because the timing of detection and the pattern of distribution of L2 and pseudogenome in the cytoplasmic vesicles and nucleus were coincident, the data depicting the pseudogenome trafficking are not shown here.

Viral Pseudogenome and L2 Localize Adjacent to ND10. It was apparent that after their entry into the nucleus the viral components were distributed in a punctate pattern reminiscent of the L2 localization at ND10 observed after expression of *de novo* synthesized protein, although in this instance the L2 protein is derived from input virions. To obtain the maximum nuclear signal, we used the 48-h time point to examine the distribution

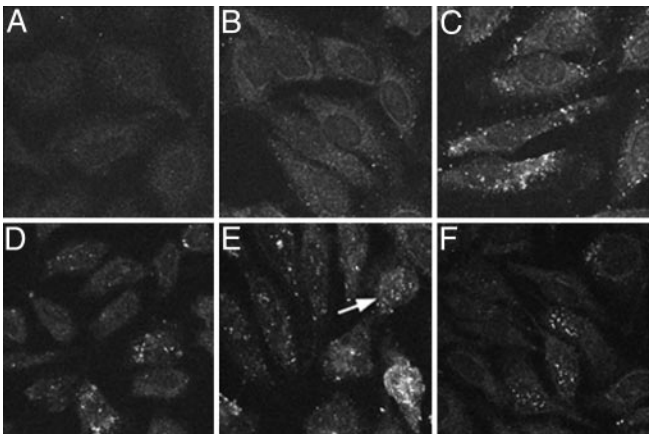

Fig. 2. Time course of viral uncoating. The appearance of the HA epitope on the L2 protein was monitored by confocal microscopy. Pseudovirions were added to HeLa cells for various times, fixed, and stained with an anti-HA monoclonal antibody that was then detected with FITC-conjugated donkey anti-mouse IgG. (*A*) The cells processed identically, but with no added pseudovirus. (*B*) Two hours, (*C*) 6 h, (*D*) 16 h, (*E*) 20 h, and (*F*) 24 h after pseudovirus addition. Note the cell in *E* (arrow) with nuclear accumulation of the L2 protein. Three similar cells are obvious in the center of *F*.

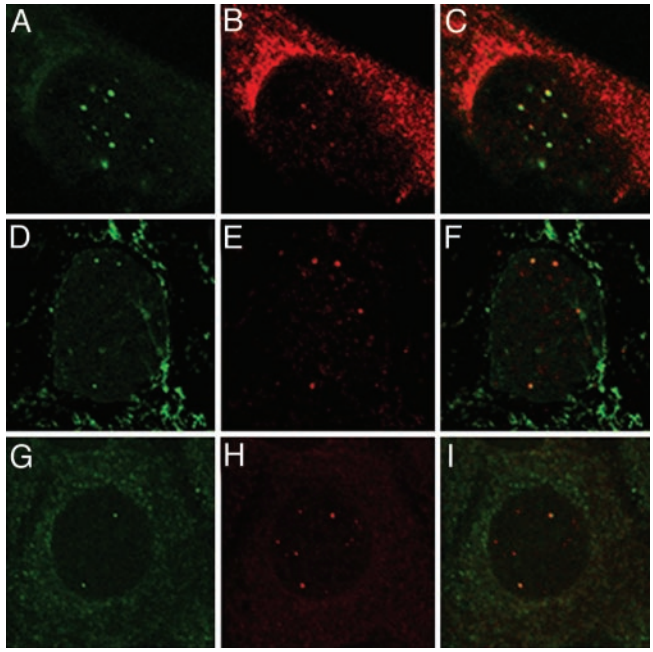

Fig. 3. L2 and the viral pseudogenome localize at ND10. HeLa cells were allowed to internalize L1 + L2-HA pseudovirions that were assembled in the presence of 20 mM BrdUrd. Forty-eight hours postentry, the cells were fixed and processed for BrdUrd detection coincident with detection of the HA epitope and PML protein. *A–C* show the same cell, processed for codetection of the pseudogenome and L2-HA protein. Mouse anti-BrdUrd staining is shown in the green channel (*A*) and rabbit anti-HA in the red channel (*B*). The merge is shown in *C*. *D–F* show the same field with the green channel representing the mouse anti-HA in *D*, the red channel with rabbit anti-PML in *E*, and the merge of the two in *F*. In *G–I*, the green channel (*G*) shows the mouse anti-BrdUrd staining; the red channel (*H*), rabbit anti-PML. The merge is shown in *F*.

of the pseudogenome and L2 relative to each other and then to the PML protein. The pseudogenome and L2 were colocalized (Fig. 3 *A–C*), although only a subset of the pseudogenome appeared to have associated with L2. This difference may result from a hindrance of the binding of the anti-HA polyclonal antiserum when detecting the heavily labeled DNA with the anti-BrdUrd antibody. In support of this possibility, we noticed a quenching of the anti-HA fluorescent signal during double detection versus single detection. An alternative explanation is that some pseudogenomes may not be associated with L2 in the nucleus, or that after entry into the nucleus, some of the L2 protein may be degraded. When we examined the localization of the viral components relative to PML, we found that L2 was clearly localized adjacent to PML, indicating residence in the vicinity of ND10 (Fig. 3 *D–F*). The pseudogenome showed a similar localization (Fig. 3 *G–I*). The accumulation at ND10 occurred with each of several packaged pseudogenomes that we examined, indicating a lack of DNA sequence specificity for this localization. Additionally, similar L2 and pseudogenome localizations were seen in other tested cell lines (C127, 1634, HaCaT, and murine fibroblasts). On average, 60% of the cells that have detectable nuclear L2 showed some colocalization with PML. The colocalization of the pseudogenome and PML was slightly higher, with an average just over 70%.

PV Infection Is More Efficient in PML+ Cells. The colocalization of both L2 and the pseudogenome near ND10 led us to wonder whether the presence of ND10 might play a role in the establishment of infection. Because PML is required for ND10 formation, we compared PML−/− cells (transfected with empty

vector, Hemp cells) with those expressing PML (PML−/− cells transfected with the *PML3* gene, Hp3 cells) for their ability to support early events in infection, using a BPV pseudovirus with an encapsidated GFP expression plasmid. The number of transduced GFP-expressing cells was found to be strikingly higher in the PML-expressing transfectants compared to the control cells (Fig. 4*A*). We consistently detected an order of magnitude difference in the number of infected cells between the PML-expressing Hp3 cells and the PML-null, Hemp cells, based on GFP expression above threshold. The observed differences in infection were not the result of delayed kinetics in the PML null cells, as confirmed by monitoring the GFP fluorescence for up to 10 days after pseudoviral infection. Both cell types showed peak GFP expression by 4 days postinfection that gradually decreased over time (Fig. 4*B*).

To confirm that the observed difference was relevant to infection by authentic virus, we also assayed the ability of the cells to support early infection by authentic BPV virions, isolated from bovine warts, as determined by quantification of early spliced mRNA. The E5 mRNA transcribed from the P2443 promoter and spliced from nucleotides 2505–3225 was monitored by using a splice-specific real-time QRT-PCR assay. By this quantitative assay, early mRNA expression via authentic virus was 10-fold lower in PML−/− cells than in PML3 reconstituted cells (Fig. 4*C*), as had been seen with GFP protein expression via pseudoviral transduction. A second splice-specific assay for 864-3225 mRNA gave similar results (data not shown).

L2 Is Diffusely Nuclear in PML−/− Cells. We also examined the localization of L2 and pseudogenome in the Hemp and Hp3 cells. In the PML-expressing Hp3 cells, both the pseudogenome and L2 were found adjacent to ND10, as expected (Fig. 5 *A–F*). However, in the cells lacking PML, the distribution of L2, although nuclear, was more diffuse (Fig. 5*G*), in contrast to the pseudogenome, which still exhibited a punctate pattern that did not differ sharply from that in the PML-expressing cells (Fig. 5*H*). It is likely that this pattern represents the detection of randomly distributed single copies of the highly BrdUrd-labeled pseudogenome. The appearance of nuclear staining in the Hemp occurred with the same kinetics as that in the Hp3 cells (data not shown). The results, therefore, suggested that the import of L2 and pseudogenome into the nucleus was unaffected in the PML-null Hemp cells, whereas the nuclear colocalization of L2 and pseudogenome appeared to be largely PML-dependent.

Discussion

Previous studies have shown that PVs traverse the endosomal route during their entry process (18–20), and that infection can be disrupted by lysosomotropic agents (18, 19). Here, we have determined that during the establishment of infection, uncoating occurs in a vesicular cytoplasmic compartment, L2, and that the associated viral genome colocalizes adjacent to ND10 by a mechanism independent of the viral DNA sequence, and that efficient transcription of the genome requires ND10 or PML. The nuclear entry of L2 and the genome does not depend on ND10 or PML. These observations were made by using PV pseudoviruses whose binding and uptake by cells parallel that of authentic PVs, and the dependence of efficient transcription on ND10 or PML was confirmed with authentic BPV virions.

PVs are taken up with surprisingly slow kinetics (19, 30), and the virus can still be substantially neutralized hours after binding the cell surface (31–33). Using a nested RT-PCR assay, we found that spliced mRNA was first detectable at 12 h postinfection (18). However, this time point represents the leading edge of infection, because less sensitive but more quantitative techniques show a gradual increase in the number of viral transcripts in the days after infection. Consistent with these kinetics, we found here that vesicular uncoating, as measured by exposure of both the pseudoviral genome and an HA epitope fused to the L2 protein, was first detected 6 h postinfection. The accumulation of both L2 and pseudogenome at ND10 was first detectable ≈12 h after the initial vesicular uncoating. However, because transcripts are detectable by this time, we expect that the viral

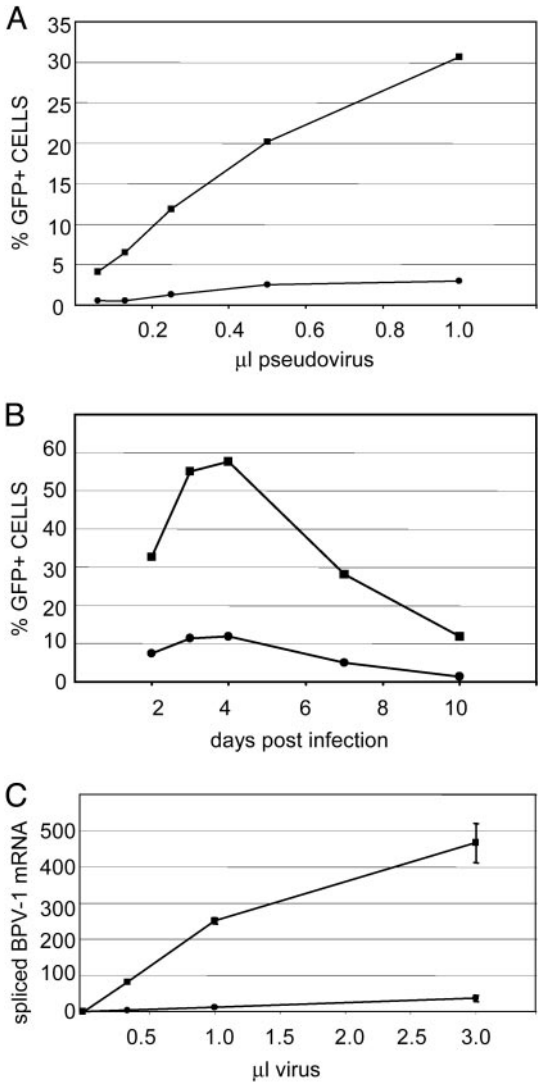

Fig. 4. PML−/− cells are neither efficiently transduced by PV pseudovirus nor infected with BPV virions. (*A*) The transduction of the PML−/− cells, Hemp (closed circles), or PML3-expressing transfectants, HP3 (closed squares). BPV L1 + L2 pseudovirus with a packaged GFP expression plasmid was added to cells for 48 h (1.0 μl of pseudovirus stock is equivalent to 200 ng of particles). GFP expression was determined by flow cytometric analysis. Marker boundaries were set such that untransduced control cells showed <1.0% fluorescent cells. Shown is a representative experiment of five separate experiments performed on different days. *B* shows the real-time QRT-PCR analysis quantifying the spliced E5 mRNA. BPV1 virions, derived from bovine warts, were added to cells for 72 h. RNA was extracted and analyzed by a real-time QRT-PCR assay specific for spliced mRNAs from nucleotides 2505–3225, as described in *Materials and Methods.* Quantities of mRNA are expressed as femtogram of the DNA standard. Each data point is the average of three independent infections. The results with the Hemp cells are designated with closed circles and those of the HP3 cells with closed squares (1.0 μl of virus stock is equivalent to 250 ng of particles). (*C*) The time course of PV pseudovirus transduction of Hemp or HP3 cells. GFP expression driven from the plasmid packaged in BPV L1 + L2 pseudovirions was monitored for 10 days postinfection. Pseudovirions were added to cells. Cells were harvested at the indicated day and processed for flow cytometric analysis. Marker boundaries were set such that untransduced control cells showed <1.0% fluorescent cells.

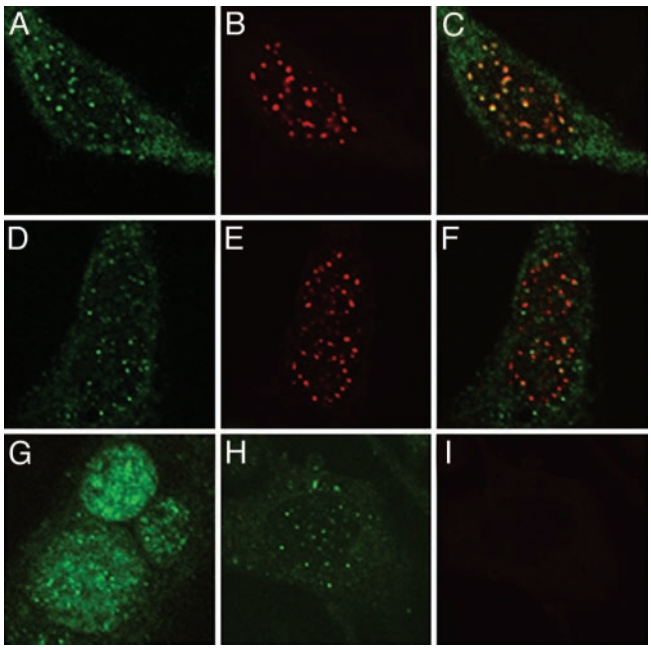

Fig. 5. L2 and pseudogenome localization in HP3 and Hemp cells. Cells were allowed to internalize L1 + L2-HA pseudovirions that were assembled in the presence of 20 mM BrdUrd. Forty-eight hours postentry, the cells were fixed and processed for BrdUrd detection coincident with detection of the HA epitope and PML protein. (*A–C*) Staining of the PML3-expressing HP3 cells to show the distribution of the L2 protein, detected with an anti-HA monoclonal antibody, is shown in *A*; the rabbit anti-PML staining is shown in *B*; and the merge of the two channels is shown in *C*. *D–F* also show the HP3 cells. *D*, mouse anti-BrdUrd detection; *E*, anti-PML staining; and *F*, the merge. Staining of the pseudovirion components in Hemp cells is shown in *G–I*. *G*, the more diffuse localization of L2, represented by anti-HA detection; *H*, the pattern of the BrdUrd-labeled pseudogenome; *I*, the anti-PML staining of these cells demonstrating the lack of expression of this protein.

components are actually delivered to ND10 somewhat earlier but at levels too low to be detected by the anti-HA or anti-BrdUrd antibodies.

PML is the critical organizing protein of ND10. It appears to be essential for the proper localization of all other ND10-associated proteins, because ND10s are not observed in a PML−/− cell line, and introduction of the PML protein results in *de novo* formation of ND10 (34). Here, we observed a dramatic increase in the efficiency of early viral gene expression in cells with PML/intact ND10 when we compared PML−/− cells with cells stably transfected with a PML expression plasmid. These results implicate ND10, or PML, in the positive regulation of PV gene expression, although it is not possible to conclude whether the observed effects result from the PML protein *per se* or from the presence of intact ND10.

Several other DNA viruses also initiate their synthetic processes in the vicinity of ND10 (reviewed in refs. 7 and 8), but a role for ND10 in their transcription has not been fully established. For example, although parental human cytomegalovirus and simian virus 40 genomes are found in association with ND10 (35–37), the levels of viral RNA were unaltered in cells lacking PML and ND10 (37, 38), in contrast to our findings for PV.

The mechanism by which PVs accumulate near ND10 may also be distinct. Our observation that PV-specific DNA sequences were not required for ND10 localization strongly suggests that the presence of pseudogenomes at ND10 depends only on the L2 protein, which binds viral genomes or pseudogenomes by a DNA sequence-independent mechanism and localizes to ND10 when synthesized in the absence of other viral sequences. For HSV-1, by contrast, a specific viral DNA sequence, OriS, in addition to the viral immediate-early proteins ICP4 and ICP27, was required to observe ND10 localization and transcript accumulation (39, 40).

The positive function we have identified for PML or ND10 in PV infection also contrasts with the postulated negative role for ND10 in many other viral infections. Most DNA viruses have evolved a means to disrupt ND10 soon after the immediate early transcription has begun. Conversely, many ND10 proteins, including PML, are induced after IFN treatment (reviewed in ref. 41). These observations have led to the proposal that ND10 may play a role in the antiviral action of IFN, and that viral-mediated disruption of ND10 is an example of viral antagonism of the antiviral IFN system. PVs have not been demonstrated to disrupt ND10, but L2 has been shown to more modestly affect the structure by increasing the local Daxx concentration and decreasing Sp100 at ND10 (42).

The model that we suggest is an L2-dependent chaperoning of packaged DNA that deposits both the L2 protein and the DNA at ND10, which then results in increased viral transcription. Capsid proteins have not previously been implicated in the deposition of a viral genome at ND10. The example of the human cytomegalovirus (HCMV) tegument protein, pp71, which functions to activate viral immediate early transcription (43) and has been shown to be necessary for genome localization and transcription at ND10 (35), may have some similarities, but, as previously mentioned, the absence of ND10 does not affect the level of HCMV transcripts (38). L2 is not known to possess any transcriptional activity, which suggests that its main function in this process is to localize the DNA to a site that favors transcription. However, a possible role for L2 in binding and/or recruitment of transcription factors has not been rigorously ruled out.

The precise function of PML/ND10 that enhances PV transcription is unclear. ND10s have been proposed to act as nuclear sensors that can detect exogenously introduced proteins (6, 44). It has been demonstrated that ND10s assemble at precise subnuclear locations frequently adjacent to compartments that participate in RNA processing, including Cajal bodies, cleavage bodies, and SC35-positive splicing sites (45, 46). This proximity suggests that ND10 could also play a part in such events. The role of ND10 in active cellular transcription is uncertain and has been widely disputed (see ref. 47 for review). Several lines of evidence support a role for ND10 in cellular transcriptional regulation (48). Newly synthesized RNA is associated with the periphery of ND10, and many transcriptional regulators have been shown to biochemically interact with PML (49–51). However, other studies have found no association of nascent RNA, active transcription, or general transcription factors at ND10 (45, 49, 52). Kiesslich *et al.* (53) confirmed that in nonsynchronized cells the majority of nascent RNA was not associated with ND10. However, they did find that the majority of active mRNA transcription sites overlapped with ND10 during the G_1 phase of the cell cycle and in cells treated with exogenous IFN-γ, suggesting that, although basal activity may not require the presence of ND10, up-regulated transcription may. The introduction of viral DNA during a viral infection could constitute an example of this induced activity.

If ND10s do act as nuclear sensors of foreign protein, it is possible that the homing of L2 to these sites may result from this function. However, it has been demonstrated (54, 55) that *de novo* synthesized L2 is localized to ND10, and L2 in natural human PV lesions is similarly found there (42). Therefore, it seems more likely that L2 has a specific mechanism for its association at this domain, whether the protein is imported into the nucleus after its exogenous introduction into the cell as part of the virion during the early phases of viral infection or after its *de novo* synthesis at later stages of infection. However, in

contrast to *de novo* synthesis, where L2 is often seen to colocalize with all of the ND10s within a cell, in the current study we found only a minority of ND10s in any cell have associated L2 or genome. It is not likely to result from differences in affinity for particular PML isoforms (56), because it is also observable in the Hp3 cells, which express only the PML3 splice variant.

It is well established that the L2 protein is critical for the assembly and/or transmission of infectious virions. L2 has been shown to be necessary for DNA packaging in some PV types (16, 57, 58) and is likely to have additional roles during infection. As envisioned in the proposed model, L2 has the novel postentry role of delivering the genome to ND10, where it can be efficiently transcribed, in contrast to other nuclear DNA viruses, which initially localize to ND10 and then induce ND10 dissolution.

We thank Janet DiPasquale and Jesse Ventura for expert technical assistance and Pier Paulo Pandolfi (Memorial Sloan–Kettering Cancer Center, New York) for the gift of the PML−/− fibroblasts.

1. Whittaker, G., Kann, M. & Helenius, A. (2000) *Annu. Rev. Cell Dev. Biol.* **16,** 627–651.
2. Rabe, B., Vlachou, A., Pante, N., Helenius, A. & Kann, M. (2003) *Proc. Natl. Acad. Sci. USA* **100,** 9849–9854.
3. Clever, J., Yamada, M. & Kasamatsu, H. (1991) *Proc. Natl. Acad. Sci. USA* **88,** 7333–7337.
4. Greber, U., Suomalainen, M., Stidwell, R. P., Boucke, K., Ebersold, M. & Helenius, A. (1997) *EMBO J.* **16,** 5998–6007.
5. Ojala, P., Sodeik, B., Ebersold, M., Kutay, U. & Helenius, A. (2000) *Mol. Cell. Biol.* **20,** 4922–4931.
6. Maul, G. G., Negorev, D., Bell, P. & Ishov, A. M. (2000) *J. Struct. Biol.* **129,** 278–287.
7. Everett, R. (2001) *Oncogene* **20,** 7266–7273.
8. Maul, G. (1998) *BioEssays* **20,** 660–667.
9. Maul, G. & Everett, R. (1994) *J. Gen. Virol.* **75,** 1223–1233.
10. Guldner, H., Szostecki, C., Grotzinger, T. & Will, H. (1992) *J. Immunol.* **149,** 4067–4073.
11. Korioth, F., Gieffers, C., Maul, G. & Frey, J. (1995) *J. Cell Biol.* **130,** 1–13.
12. Koken, M., Puvion-Dutilleul, F., Guillemin, M., Viron, V., Linares-Cruz, G., Stuurman, N., de Jong, L., Szostecki, C., Cairo, F., Chomienne, C., *et al.* (1994) *EMBO J.* **13,** 1073–1083.
13. Maul, G., Yu, E., Ishov, A. & Epstein, A. (1995) *J. Cell Biochem.* **59,** 498–513.
14. Lowy, D. R. & Howley, P. M. (2001) in *Fields Virology*, eds. Knipe, D. M. & Howley, P. M. (Lippincott Williams & Wilkins, Baltimore), Vol. 2, pp. 2231–2264.
15. Zhou, J., Stenzel, D. J., Sun, X. Y. & Frazer, I. H. (1993) *J. Gen. Virol.* **74,** 763–768.
16. Roden, R. B., Greenstone, H. L., Kirnbauer, R., Booy, F. P., Jessie, J., Lowy, D. R. & Schiller, J. T. (1996) *J. Virol.* **70,** 5875–5883.
17. Roden, R. B., Day, P. M., Bronzo, B. K., Yutzy, W. H., IV, Yang, Y., Lowy, D. R. & Schiller, J. T. (2001) *J. Virol.* **75,** 10493–10497.
18. Day, P. M., Lowy, D. R. & Schiller, J. T. (2003) *Virology* **307,** 1–11.
19. Selinka, H. C., Giroglou, T. & Sapp, M. (2002) *Virology* **299,** 279–287.
20. Bousarghin, L., Touze, A., Sizaret, P. Y. & Coursaget, P. (2003) *J. Virol.* **77,** 3846–3850.
21. Buck, C. B., Pastrana, D. V., Lowy, D. R. & Schiller, J. T. (2004) *J. Virol.* **78,** 751–757.
22. Pastrana, D. V., Buck, C. B., Pang, Y. Y., Thompson, C. D., Castle, P. E., FitzGerald, P. C., Kruger Kjaer, S., Lowy, D. R. & Schiller, J. T. (2004) *Virology* **321,** 205–216.
23. Wang, Z. G., Delva, L., Gaboli, M., Rivi, R., Giorgio, M., Cordon-Cardo, C., Grosveld, F. & Pandolfi, P. P. (1998) *Science* **279,** 1547–1551.
24. Khan, S. G., Muniz-Medina, V., Shahlavi, T., Baker, C. C., Inui, H., Ueda, T., Emmert, S., Schneider, T. D. & Kraemer, K. H. (2002) *Nucleic Acids Res.* **30,** 3624–3631.
25. Baker, C. C. & Caleb, C. (1995) in *Human Papillomaviruses 1995* (Los Alamos Natl. Lab., Los Alamos, NM), pp. III3–20.
26. Yang, Y. C., Okayama, H. & Howley, P. M. (1985) *Proc. Natl. Acad. Sci. USA* **82,** 1030–1034.
27. Merle, E., Rose, R., LeRoux, L. & Moroianu, J. (1999) *J. Cell Biochem.* **74,** 628–637.
28. Nelson, L., Rose, R., LeRoux, L., Lane, C., Bruya, K. & Moroianu, J. (2000) *J. Cell Biochem.* **79,** 225–238.
29. Liu, W. J., Gissmann, L., Sun, X. Y., Kanjanahaluethai, A., Muller, M., Doorbar, J. & Zhou, J. (1997) *Virology* **227,** 474–483.
30. Selinka, H. C., Giroglou, T., Nowak, T., Christensen, N. D. & Sapp, M. (2003) *J. Virol.* **77,** 12961–12967.
31. Christensen, N. D., Cladel, N. M. & Reed, C. A. (1995) *Virology* **207,** 136–142.
32. Culp, T. D. & Christensen, N. D. (2003) *J. Virol. Methods* **111,** 135–144.
33. Culp, T. D. & Christensen, N. D. (2004) *Virology* **319,** 152–161.
34. Ishov, A. M., Sotnikov, A. G., Negorev, D., Vladimirova, O. V., Neff, N., Kamitani, T., Yeh, E. T., Strauss, J. F., III, & Maul, G. G. (1999) *J. Cell Biol.* **147,** 221–234.
35. Ishov, A. M., Vladimirova, O. V. & Maul, G. G. (2002) *J. Virol.* **76,** 7705–7712.
36. Ahn, J. H., Jang, W. J. & Hayward, G. S. (1999) *J. Virol.* **73,** 10458–10471.
37. Tang, Q., Bell, P., Tegtmeyer, P. & Maul, G. G. (2000) *J. Virol.* **74,** 9694–9700.
38. Marshall, K. R., Rowley, K. V., Rinaldi, A., Nicholson, I. P., Ishov, A. M., Maul, G. G. & Preston, C. M. (2002) *J. Gen. Virol.* **83,** 1601–1612.
39. Sourvinos, G. & Everett, R. D. (2002) *EMBO J.* **21,** 4989–4997.
40. Tang, Q., Li, L., Ishov, A. M., Revol, V., Epstein, A. L. & Maul, G. G. (2003) *J. Virol.* **77,** 5821–5828.
41. Regad, T. & Chelbi-Alix, M. K. (2001) *Oncogene* **20,** 7274–7286.
42. Florin, L., Schafer, F., Sotlar, K., Streeck, R. E. & Sapp, M. (2002) *Virology* **295,** 97–107.
43. Bresnahan, W. A. & Shenk, T. E. (2000) *Proc. Natl. Acad. Sci. USA* **97,** 14506–14511.
44. Tsukamoto, T., Hashiguchi, N., Janicki, S. M., Tumbar, T., Belmont, A. S. & Spector, D. L. (2000) *Nat. Cell Biol.* **2,** 871–878.
45. Grande, M. A., van der Kraan, I., van Steensel, B., Schul, W., de The, H., van der Voort, H. T., de Jong, L. & van Driel, R. (1996) *J. Cell Biochem.* **63,** 280–291.
46. Shiels, C., Islam, S. A., Vatcheva, R., Sasieni, P., Sternberg, M. J., Freemont, P. S. & Sheer, D. (2001) *J. Cell Sci.* **114,** 3705–3716.
47. Borden, K. L. (2002) *Mol. Cell. Biol.* **22,** 5259–5269.
48. Zhong, S., Salomoni, P. & Pandolfi, P. P. (2000) *Nat. Cell Biol.* **2,** E85–E90.
49. Boisvert, F. M., Hendzel, M. J. & Bazett-Jones, D. P. (2000) *J. Cell Biol.* **148,** 283–292.
50. LaMorte, V. J., Dyck, J. A., Ochs, R. L. & Evans, R. M. (1998) *Proc. Natl. Acad. Sci. USA* **95,** 4991–4996.
51. Tashiro, S., Muto, A., Tanimoto, K., Tsuchiya, H., Suzuki, H., Hoshino, H., Yoshida, M., Walter, J. & Igarashi, K. (2004) *Mol. Cell Biol.* **24,** 3473–3484.
52. Wang, J., Shiels, C., Sasieni, P., Wu, P. J., Islam, S. A., Freemont, P. S. & Sheer, D. (2004) *J. Cell Biol.* **164,** 515–526.
53. Kiesslich, A., von Mikecz, A. & Hemmerich, P. (2002) *J. Struct. Biol.* **140,** 167–179.
54. Day, P. M., Roden, R. B., Lowy, D. R. & Schiller, J. T. (1998) *J. Virol.* **72,** 142–150.
55. Heino, P., Zhou, J. & Lambert, P. F. (2000) *Virology* **276,** 304–314.
56. Fagioli, M., Alcalay, M., Pandolfi, P. P., Venturini, L., Mencarelli, A., Simeone, A., Acampora, D., Grignani, F. & Pelicci, P. G. (1992) *Oncogene* **7,** 1083–1091.
57. Stauffer, Y., Raj, K., Masternak, K. & Beard, P. (1998) *J. Mol. Biol.* **283,** 529–536.
58. Zhao, K. N., Sun, X. Y., Frazer, I. H. & Zhou, J. (1998) *Virology* **243,** 482–491.